

## SEISMOGRAM ANALYSIS OF EARTHQUAKES IN SUMATRA-JAVA AT HYB OBSERVATORY STATION

**B.J. Santosa\***

Physic Department,  
Faculty of Mathematics and Natural Science  
Institute Teknologi of Surabaya, Indonesia

Received: 13 Pebruari 2012. Accepted: 13 April 2012. Published: Juli 2012

### ABSTRAK

Dalam penelitian ini struktur bumi di bawah lempeng Lautan Hindia Timur Laut dikaji melalui analisis seismogram atas seismogram gempa-gempa bumi yang terjadi di Sumatra dan direkam di stasiun observasi HYB, India. Analisis seismogram dilaksanakan dalam domain waktu dan ketiga komponen-komponen Kartesian secara simultan. Perbandingan seismogram menunjukkan bahwa model bumi global PREM memberikan seismogram sintetik yang menyimpang dari seismogram terukur dan waktu tiba gelombang S yang lebih lambat dibandingkan waktu tiba terukur. Untuk mencapai pencocokan seismogram, gradient  $\beta_n$  di *upper mantle* diubah dari positif menjadi negative, sebagaimana dinyatakan dalam model bumi PREMAN, dan koreksi kecepatan positif ditambahkan pada koefisien-koefisien kecepatan orde nol pada struktur kecepatan S dalam semua lapisan mantel bumi. Pengepasan yang bagus dicapai pada gelombang ruang S, gelombang permukaan Love dan Rayleigh, begitu juga dengan gelombang terpantul inti bumi ScS dan ScS2.

### ABSTRACT

In this research, the earth structure beneath North East Indian Ocean plates is investigated using waveform analysis of Sumatra's earthquakes recorded in HYB station. Seismogram analysis was conducted in the time domain and three Cartesian components simultaneously. The seismogram comparison shows that the global earth mantle of PREM provides deviating synthetic seismogram and has later arrival times than those from the measurement. To achieve the seismogram fitting, the gradient  $\beta_n$  in the upper mantle layers was altered to positive from its negative slope as stated in the PREM model, and positive corrections are added to the zero order of polynomials coefficients of S velocity structure in all earth mantle layers. The excellent fitting, as well as travel time and waveform, were achieved on the S wave, Love and Rayleigh surface waves, as well as the ScS and ScS2 core reflected waves.

© 2012 Physic Department FMIPA UNNES Semarang

**Keywords:** Seismogram analysis; Vertical anisotropy; Positive velocity anomaly

### INTRODUCTION

Geological condition of the research area is as follows: a collision occurred between the Indian Ocean plate and the Asia plate; which occurs until now, resulting of a subduction structure on the west coast of Sumatra and the south coast of Java. In Java, the subduction zone is going into north direction and it turned into northwest direction in Sumatra area. It cau-

ses the huge fault plane along Sumatra Island parallel to the direction of subduction field in Sumatra area. This fault plane is along the Bukit Barisan Mountain Range. The continuous collision between the oceanic plate and continent plate causes the increasing stress in the rock constituted continental plate; and if the strain exceeds  $10^{-4}$ , the rock will begin to crash, and it initiates an earthquake. The rock volume which experienced a dislocation will affect the amount of energy released by the earthquake, and if the earthquake is shallow one on the oceanic plate, it also enables a formation of Tsunami. The oceanic plates still move until now with an

---

\*Alamat Korespondensi:  
Jl. Arif Rahman 1, Surabaya 60111  
E-mail: bjs@physics.its.ac.id

average velocity of 14 cm/year, resulting the great tectonic earthquakes. It is characterized by a great number of earthquakes in this zone. The seismogram result of some earthquakes that occur in this subduction area and in the fault plane of Sumatra Island will be analyzed in the time domain and three Cartesian components in HYB observatory station, India.

Recent tomography methods use information of the arrival-time data (Hall, 2002; Replumaz et al., 2004; Engdahl et al., 1998; Vasco et al., 1995; Zhou, 1996; Grand et al., 1997; van der Hilst et al., 1997; Boschi and Dziewonski, 1999; Zhao, 2001, 2004; Garnero, 2000; Nettles and Dziewonski, 2008) which is extracted from the seismogram time series, based on the manual and automatic methods. Overall, I mention these methods as a time based tomography.

The other tomography methods also used the separated waveform of S and surface wave (Panning and Romanowicz, 2008; Takeuchi, 2007), while this research analyzed the entire seismogram from S, Love and Rayleigh waves to the deep core reflected wave ScS and multiple.

The waveform tomography is different from the general method of seismology in two aspects:

1. The data input is composed of the seismogram of three components in the time domain.
2. The numeric method used is based on the full wave equation.

The above mentioned features creating a waveform tomography without any approach; and consequently, give a better resolution than the travel time at some points in the seismogram time series. The data set analyzed in this research is waveforms in seismogram, instead the travel time data. Although the data set used by other seismologists reaches a number of millions, the travel time contains just a little information in the seismogram time range. Whereas the waveform of the S wave, the Love and Rayleigh surface waves in three Cartesian components simultaneously and also the core reflected wave phase ScS and ScS<sub>2</sub>, process all information contained in the seismogram completely. Takeuchi (2007) has also used the method of waveform tomography, but only on the seismogram of transversal component only.

The P wave velocity structure in this area in the previous seismology research (Replumaz et al., 2004; Grand et al., 1997; van der

Hilst et al., 1997) has been interpreted using travel time data, where the travel time data is supplied by International Seismological Center (ISC). The previous earth model was obtained by inverting the travel-time data of the P wave directly, amounting to  $8 \times 10^6$ , the phase of reflected wave pP amounting to  $0.6 \times 10^6$ , and biased in the earth core PKP nearly amounting to  $1 \times 10^6$ . The amount of data collected from 300.000 earthquakes from the interval 1/1/1964 until to 31/12/2000 and also a small amount of data of the absolute difference of the travel times PP-P, PKP-Pdiff is accurately measured by the cross-correlation of waveform taken from the broad-band digital data (Gomer and Okal, 2003). The forward waveform modeling has complemented the detail about the structural features in the same vein with the small heterogeneity pattern refer to the last reviews, (Zhao, 2001; 2004). This study has widely increased our knowledge about the structure and dynamics of the deep interior of the earth. The subducted layers of lithosphere and the expanded ocean-mantle become the two mutually-complemented features in the mantle convection.

The objective of this research is to investigate the earth structure beneath North East Indian Ocean using seismogram analysis and fitting where the earthquakes occurred in Sumatra and Java and recorded in the observatory station of HYB, India. The wave paths from earthquakes hypocenter to observatory station traverse the earth structure beneath Oceanic plates of Bengal Ocean where the wave rays propagate into the back structure of the subduction field.

## METHOD

The position of the HYB observatory station and the epicenters of earthquakes and the vertical projection of the wave paths from the earthquakes hypocenter to the observatory station are presented in Fig. 1. The three dimensional location of the earthquakes is presented in Table 1.

The data set used is the seismogram comparison between the measured and the synthetic seismogram. The synthetic seismogram is calculated using the GEMINI (Greens Function of the earth by Minor Integration) method (Dalkolmo, 1993; Friederich and Dalkolmo, 1995), which is equivalent with the Normal Mode, but the highest frequency can be set arbitrary.

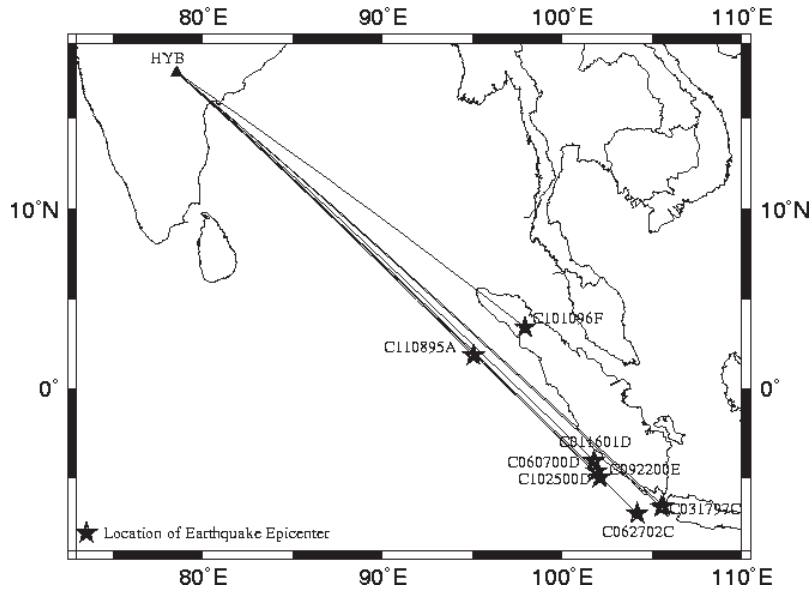


**Figure 1.** The vertical projection of the wave paths from the earthquakes hypocenter to the HYB seismology observatory station

**Table 1.** The Codes and locations of earthquakes in Sumatra and Java that are analyzed at HYB station

<i>Earthquake Code</i>	<i>Latitude °</i>	<i>East Longitude °</i>	<i>Depth km</i>
C101096F	3.44	97.04	22.8
C110895A	1.85	95.06	29.6
C011601D	-4.02	101.78	20
C060700D	-4.61	101.9	16.6
C092200E	-4.96	102.1	33
C102500D	-6.55	105.63	45.6
C031797C	-6.61	105.51	42.7
C062702C	-6.96	104.18	15

The GEMINI program calculates the Minors of the Green functions for a given earth model (e.g. the vertical anisotropic PREM (Preliminary Reference Earth Model, Dziewonski and Anderson, 1981), hereafter we call as PREMAN) and for a certain depth of the earthquake source. The Greens function is integrated from the deepest point in the wave trajectory (reflected point) to the source depth, denoted as  $g_1$  and  $g_2$  and from earth surface to source depth, denoted as  $w_1$  and  $w_2$ , by fulfilling the boundary conditions at those points and at the earth surface. The expansion is written using the independent variable, that is, the complex frequency ( $\omega+i\sigma$ ), to avoid the time aliasing. The earthquake tensor moment detailed in the third line of the CMT (Centroid Moment Tensor) solution (Dreger, 2002), is used to calculate the right side of the motion equation system. The motion equation system forms a linear

equation system, whereas the left side consist of Greens functions, and the right side is expanded in the spherical harmonic function with tensor moment coefficients. The linear equation system is solved using the Cramer rule. The coefficients for the Minors of Greens functions are then obtained.

The coordinate of the earthquake source is put at the North Pole, and the coordinate of the observatory stations is calculated in the forms of epicentral and azimuth angles. The spherical harmonic function is developed with both of the angle values. The DISPEC program (belongs to the GEMINI Package) reads the Greens function produced by GEMINI program and forms a multiplication with the spherical harmonic coefficients from the Cramer solution. The spherical harmonics were evaluated using the epicentral and azimuth angles. The DISPEC program ends by summing them up.

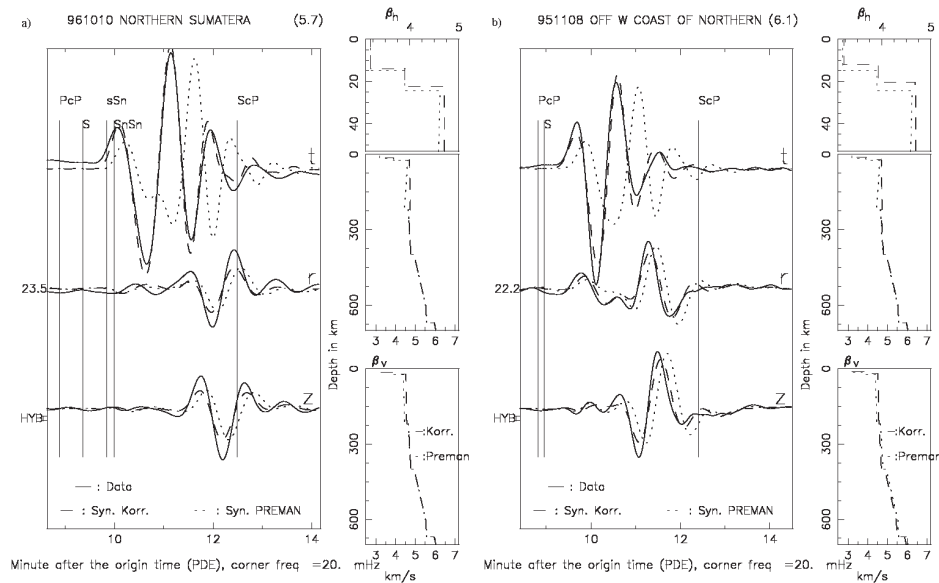


**Figure 2.** The seismogram fitting and analysis of the earthquakes in North Sumatra in HYB station: a) C101096F; b) C 110895A

The result is the synthetic seismogram in the complex frequency domain. The MONPR program (GEMINI package) transforms the synthetic seismogram from the complex frequency domain into the time domain. The measured and synthetic seismograms are subject to a Butterworth low pass filter to get a simpler waveform analysis. The measured seismogram is subjected to the inverted response file from the seismogram equipment system. Response file is a description of the phase change and the amplification of the equipment system in the observatory. The input of the seismometer is the velocity/acceleration of the ground motion and the output is the electric voltage (mV). By applying the inversed RESPONSE filter on the measured seismogram, the comparison between the measured seismogram and the synthetic one is performed in the same unit (mm/sec).

The horizontal components of the measured seismogram should be rotated with the y-axis (North-South Canal), directed to the small arch formed by the observatory station to the earthquake source (back azimuth, see Fig. 1). It is used to decompose the complex ground motion in the 3-D space into the P-SV and SH components. Therefore, the synthetic and the measured seismograms are compared in the same unit and direction of motion.

The seismogram analysis is presented in Figure 2 and so on. Each figure contains 3 curves, where the solid curve presents the measured data. The dot curve is the synthetic seis-

mogram constructed from the PREMAN earth model, and the dot-dash curve is the synthetic seismogram constructed from corrected earth model. The velocity correction includes the changing of the  $\beta_h$  velocity gradient in the upper mantle layers into positive rather than negative as in the PREMAN. The corrections on the zero-order coefficients of the velocity polynomial function of both kinds of  $\beta$  in the mantle layers. Corrections are required to obtain a seismogram matching in all phases of the S wave and multiple, and also the surface waves of Love and Rayleigh. The correction result of the  $\beta$  velocity is presented in the right box, between the PREMAN earth model and the corrected earth model.

The first analyzed seismogram is of C101096 earthquake, North Sumatra, where hypocenters lie on the fault plane of Semangko Fault, and the ground movement due to earthquake, recorded in HYB station. Fig. 2. shows that PREMAN earth model provides the Love synthetic wave that arrives later than the measured Love, while the corrected earth model provides an excellent fitting, obtained on both kinds of the surface wave, Love and Rayleigh wave. The correction on  $\beta_h$  is stronger than the correction on  $\beta_v$ . It indicates that the Indian Ocean plate that lies behind the subduction field has a positive anomaly of the  $\beta$  velocity.

Figure 2b presents seismogram analysis and fitting of the C110895A earthquake, whose hypocenter lies on the subduction field of the Indian Ocean plate in North Sumatra and is

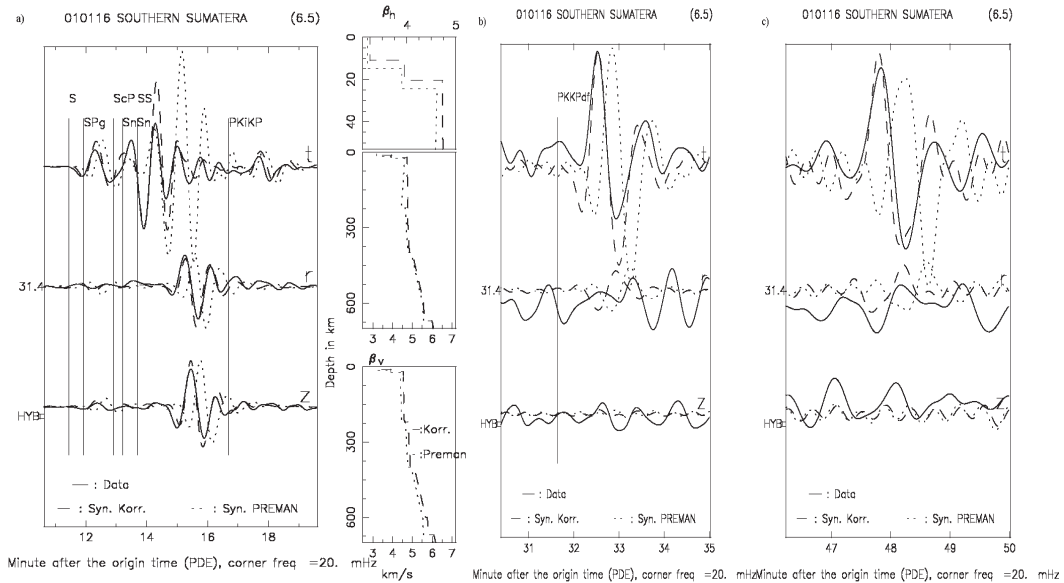


**Figure 3.** The analysis and fitting of the seismogram of C011601D earthquake on South Sumatra in station HYB: a) S, L & R; b) ScS<sub>2</sub>

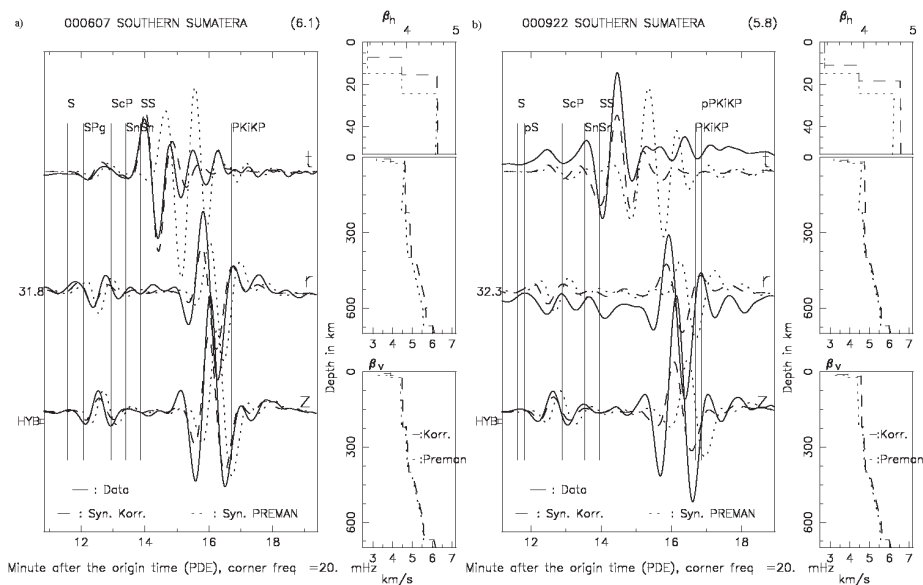


**Figure 4.** The analysis and fitting of the seismogram of earthquakes in North Sumatra in HYB station: a) C060700D; b) C092200A.

recorded in HYB station. We can see that the anomaly of  $\beta_h$  is required to find a fitting on the measured Love wave. While on the Rayleigh wave, the anomaly needed to correct  $\beta_v$  is not as strong as on  $\beta_h$ . On both of them, the seismogram data quality is poor for the time window of the core reflected wave, so the analysis was not conducted in these waves.

Figure 3 presents the seismogram fitting of the C011600A earthquake from the S and SS waves, the Love and Rayleigh surface waves, the ScS<sub>2</sub> and ScS<sub>3</sub> waves, which in their

propagation had traversed all mantle layers and earth crust four and six times, respectively. A strong positive correction on  $\beta_h$  and a weak positive correction on  $\beta_v$  in the upper mantle layers, and is continued to be positive in the mantle layers below, even until they reach the base mantle. An observation on the ScS<sub>2</sub> and ScS<sub>3</sub> waves on this small epicentral distance provides a new way to investigate the structure of the S wave velocity in the base mantle, compared with the method of the travel time differences (Souriau and Poupinet, 1991), where

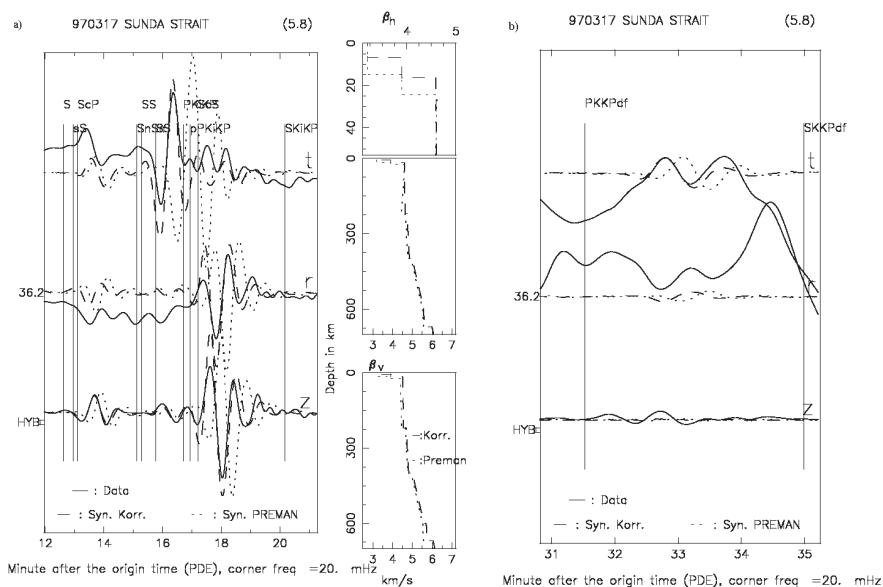


**Figure 5.** The seismogram analysis and fitting of the C031797A earthquake in Sunda Strait on HYB station: a) S, L & R; b) ScS

observatory stations are needed at epicentral distance over  $83^\circ$ .

Then, the analyzed earthquakes that occur in South Sumatra and were recorded in HYB station, as illustrated in Fig. 4a. It can be seen that, to find a fitting on the height of Love wave, the earth crust between the hypocenter of the earthquake and HYB station is thinned, as is the Ocean earth crust from PREMAN (Dziewonski and Anderson, 1981). A positive correction on  $\beta_h$  and  $\beta_v$ , occurs not only in the upper mantle, but also on the mantle layers below, to obtain a fitting on the S wave.

Next step is to obtain the Love wave fitting on the seismogram of C092200A earthquake in HYB station, as illustrated in fig. 4b, that a positive correction on velocity of both kinds of S wave occurs not only on the upper mantle layers, but also on the mantle layers below. Unfortunately, the data quality for the time piece for the ScS wave phase is poor. The analysis on four earthquakes on the coasts of South Sumatra indicates that the Indian Ocean plates have a thickness like Ocean, but with a positive anomaly of velocity S, down to the base mantle.

Figure 5 presents the seismogram analysis and fitting of the C031797A earthquake, Sunda Strait in HYB station. The fitting occurs in various wave phases, from the S wave phase, the surface waves of Love and Rayleigh, and the phase of core reflected wave ScS. These indicate that a positive correction on both kinds of  $\beta$  should be imposed on the upper

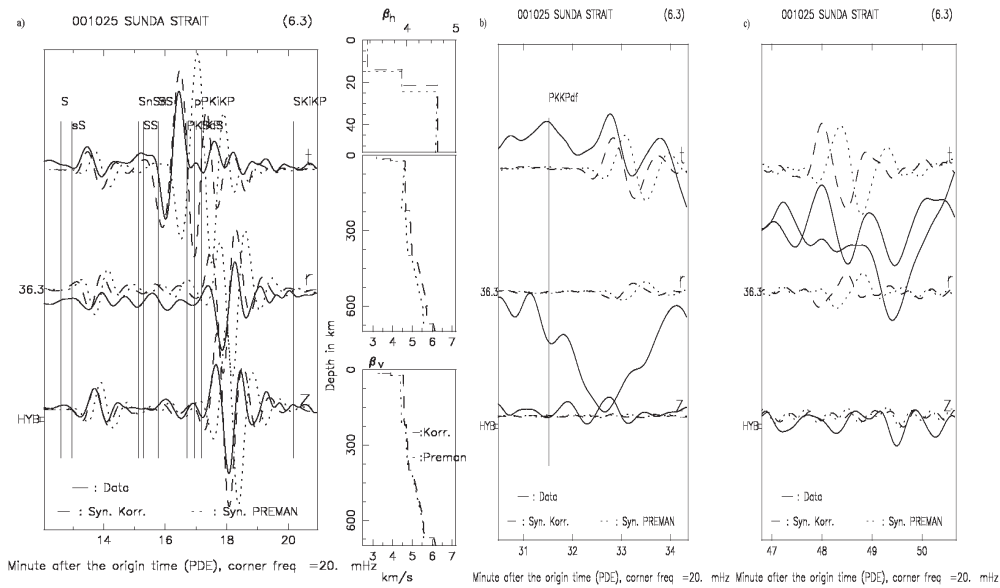
mantle layers downward until the base mantle.

Figure 6 presents the seismogram analysis and fitting of the C102500A earthquake, Sunda Strait, which is recorded in HYB station. The fitting occurs on various phases of waves, beginning from the S wave phase, the surface waves of Love and Rayleigh, core reflected ScS<sub>2</sub> and ScS<sub>3</sub> waves. These indicate that positive corrections on both kinds of  $\beta$  should be imposed on the upper mantle layers downward until the base mantle layer.

The seismogram data quality of the C062702C earthquake only shows good result on  $\$z\$$  component. Therefore, I try to find a fitting merely on z component. The fitting result indicates that the positive anomaly occurs on the mantle layers until 730 km depth. An excellent fitting on the S wave is reached, but the amplitude of the synthetic Rayleigh is weaker than that of the measured Rayleigh. It is contributed by a mistake in determining the solution of the CMT tensor (Dreger, 2002). We cannot analyze the core reflected wave, because of poor data quality.

## RESULT AND DISCUSSION

This research observed the S velocity structure beneath the Indian Ocean using seismogram analysis of earthquakes in Sumatra, which are recorded in HYB station. Wave paths from earthquakes hypocenters to observation station HYB have small azimuth degree difference; nevertheless it can still be observed



**Figure 6.** The seismogram analysis and fitting of the C102500A earthquake in Sunda Strait in HYB station: a) S, L & R; b)  $ScS_2$ ; c)  $ScS_3$

using waveform analysis method.

PREMAN earth model is presented with the vertical anisotropy features just for the upper-mantle layers. This research used waveform analysis of S body wave, Love and Rayleigh surface waves, and also core reflected wave phases. The result shows that the stated vertical anisotropy occurs not only in the upper mantle layers, but also on all earth layers until Core Mantle Boundary. Following this research, we can see that the four earthquakes analyzed indicate that the velocity anomaly of the S wave is positive for the plate structure of the Indian Ocean at HYB station. The positive anomaly occurs on all mantle layers. To find a matching for the S waves (SV and SH) on the seismogram of several earthquakes, we need a positive correction with weaker magnitude at the mantle layer until 730 km deep, and its values are different for both kinds of  $\beta$ . It indicates that the vertical anisotropy feature also occurs on the mantle layers below the upper mantle. These anisotropy features are not used in the seismology research that is based on the travel time data, because we find difficulties to observe the travel time difference between S waves on the three Cartesian-components. This result differs from result from Singh (1999) whose investigation result was based on dispersion analysis of the Rayleigh surface wave.

The fitting attainment on the phase of core reflected wave indicates that the anisotropy features continue until the earth base mantle and the anomaly of  $\beta$  is positive. The wave-

form analysis of core reflected wave phases in small epicentral distance stations is better than the method of the travel time difference of the S-SKKS wave (Wysesession et al., 1998; Souriau and Poupinet, 1991), which requires great epicentral distance stations to measure the arrival times of these waves.

## CONCLUSION

The velocity structure of the S wave behind the subduction zone and the non-tectonic areas under the Indian plates have been investigated by the seismogram analysis from the earthquakes that occurred in Sumatra, where the seismogram was recorded in HYB station, Hyderabad, India, in the time domain and the three Cartesian-components simultaneously. The data set used in this research is the seismogram comparison, making use of all information that is contained in seismogram, unlike the travel-time data set that analyzes the small portion of information that is contained in the seismogram.

The synthetic seismogram is calculated with the GEMINI method that is equivalent to the Normal Mode. To simplify the waveform, the seismograms are subjected to a low-pass filter with an angular frequency that is set on 20 mHz.

The seismogram comparison indicates that the synthetic seismogram from the earthquakes in Indonesia that was recorded in HYB calculated from the earth model PREMAN ar-

rives later than its counterpart of the measured wave phase. A correction is imposed by changing the gradient  $\beta_h$  into positive, and by imposing positive correction on the zero-order coefficients of  $\beta$  as a polynomial function on every mantle layer. A positive correction is the first correction on  $\beta_h$  to find a fitting on the Love wave, and then on  $\beta_v$  to get the fitting on the Rayleigh and S waves. A correction is also imposed on the core reflected ScS, ScS<sub>2</sub> and ScS<sub>3</sub> waves. It indicates that the vertical anisotropy feature is stronger than that stated in the PREM earth model, and also occurs in the mantle layers below the upper mantle layers.

### REFERENCE

- Boschi, L. and Dziewonski, A., 1999. High- and low-resolution images of the earth's mantle: Implications of different approaches to tomographic modeling, *Journal of Geophysical Research*, 104, 25567 – 25594.
- Dalkolmo, J., 1993. *Synthetische Seismogramme für eine sphärisch symmetrische, nichtrotierend Erde durch direkte Berechnung der Greenschen Funktion*. Diplomarbeit, Inst. für Geophys., Uni. Stuttgart
- Dreger, D.S., 2002. *Time-Domain Moment Tensor INverse Code (TDMT\_INV)*, The Berkeley Seismological Laboratory (BSL), report number 8511
- Dziewonski, A.M. and Anderson, D.L., 1981. Preliminary reference earth model. *Phys. of the Earth and Plan. Int.*, 25, 297 – 356.
- Engdahl, E.R., Van Der Hilst, R.D., & Buland, R.P., 1998. Global teleseismic earthquake relocation with improved travel times and procedures for depth determination, *Bull. Seism. Soc. Am.*, 88, 722 - 743.
- Friederich, W. and Dalkolmo, J., 1995. Complete synthetic seismograms for a spherically symmetric earth by a numerical computation of the green's function in the frequency domain. *Geophysical Journal International*, 122, 537 - 550.
- Garnero, E., 2000. Heterogeneity of the lowermost mantle. *Annu. Rev. Earth Planet. Sci.*, 28, 509–537.
- Gomer, B.M. and Okal, E.A., 2003. Multiple-ScS probing of the Ontong-Java Plateau, *Physics of the Earth and Planet Interiors*, 138, pp. 317 – 331.
- Grand, S., van der Hilst, R. & Widiyantoro, S., 1997. Global seismic tomography: a snapshot of convection in the Earth. *GSA Today*, 7, 1–7.
- Hall, R., 2002. Cenozoic geological and plate tectonic evolution of SE Asia and the SW Pacific: computer based reconstructions, model and animations, *Journal of Asian Earth Sciences*, 20, 353 – 431
- Nettles, M. and Dziewonski, A.M., 2008. Radially anisotropic shear velocity structure of the upper mantle globally and beneath North America, *Journal of Geophysical Research*, 113, B02303, doi:10.1029/2006JB004819
- Panning, M. and Romanowicz, B., 2008. A three-dimensional radially anisotropic model of shear velocity in the whole mantle. *Geophysical Journal International*, 167, pp. 361 - 379.
- Replumaz, A, Káráson, H, van der Hilst, R. D., Besse, J. & Tapponnier, P., 2004. 4-D evolution of SE Asia's mantle from geological reconstructions and seismic tomography, *Earth and Planetary Science Letters*, 221, 103 – 115
- Singh, D.D., 1999. Surface wave tomography studies beneath the Indian subcontinent, *Geodynamic*, 28, pp. 291 – 301.
- Takeuchi, N., 2007. Whole mantle SH velocity model constrained by waveform inversion based on three-dimensional Born kernels, *Geophysical Journal International*, 169, Number 3, June 2007, pp. 1153 – 1163.
- van der Hilst, R., Widiyantoro, S. & Engdahl, E., 1997. Evidence for deep mantle circulation from global tomography. *Nature*, 386, 578–584.
- Vasco, D., Johnson, L. & Pulliam, R., 1995. Lateral variations in mantle velocity structure and discontinuities determined from P, PP, S, SS, and SS-ScS travel time residuals. *J. Geophys. Res.*, 100, 24037–24059.
- Wysession, M., Lay T. & Revenaugh J., 1998. The D<sup>n</sup> discontinuity and its implications. In: Gurnis, M., Buffett, B., Knittle, K., Wysession, M. (Eds.), *The Core–Mantle Boundary*. *Am. Geophys. Union*, pp. 273–297.
- Zhao, D., 2001. Seismic structure and origin of hotspots and mantle plumes, *Earth and Planetary Science Letter*, 192, 251–265.
- Zhao, D., 2004. Global tomographic images of mantle plumes and subducting slabs: insight into deep Earth dynamics, *Physics of the Earth and Planetary Interiors*, 146, 3–34
- Zhou, H., 1996. A high-resolution P wave model for the top 1200 km of the mantle. *Journal of Geophysical Research*, 101, 27791 – 27810.